Title

Evolutionary and functional analyses reveal conserved and non-conserved functions of vertebrate RIP kinases

Authors

Elizabeth J. Fay[1], Kolya Isterabadi[1], Charles M. Rezanka[1], Jessica Le[1], Matthew D. Daugherty[1]*

Affiliations

[1]Department of Molecular Biology, School of Biological Sciences, University of California, San Diego, La Jolla, CA, 92093

* To whom correspondence should be addressed: Matthew D. Daugherty (mddaugherty@ucsd.edu)

Abstract

Receptor interacting protein kinases (RIPKs) play important roles in diverse innate immune signaling pathways. Despite this, some RIPK-associated proteins are absent in specific vertebrate lineages, suggesting that some aspects of RIPK protein function are well conserved while other functions are more evolutionarily labile. Here, we perform phylogenomic analyses of RIPK1-5 and associated proteins in vertebrates to identify RIPK functions that are well conserved, such as NF-κB signaling, and functions that have undergone pervasive gene loss, such as necroptosis. We further use functional approaches to characterize RIPK1-5 in humans and RIPK1 and RIPK3 across diverse species. Consistent with our phylogenomic inferences, we identify NF-κB as a core function of RIP kinases in humans, albeit through diverse mechanisms. We additionally identified conservation of the RIP homotypic interaction motif in RIPK1 and RIPK3, despite loss of key mediators of RIPK1/3 function in vertebrates. The preservation of this motif has also led to the conservation of NF-κB activation by RIPK1 and RIPK3, with some variation in regulatory mechanisms, from diverse vertebrate and non-vertebrate species. Altogether, these data suggest that NF-κB activation is a core, conserved

function of RIP kinases, while additional RIPK functions have been tailored to specific needs within and between species.

Introduction

Receptor-interacting protein kinases 1-5 (RIPK1-5) are a family of intracellular signaling proteins with diverse and overlapping roles in innate immunity [1, 2]. These proteins share a similar domain structure marked by a homologous N-terminal kinase domain, an intermediate domain, and a C-terminal interaction domain [3]. RIPK1-3 have all been shown to play a role in the response to pathogens through activation of the pro-inflammatory and pro-survival transcription factor NF-κB, inflammatory and non-inflammatory cell death, and type I interferon (IFN-I) signaling [2]. RIPK4 can activate NF-κB [4], but has no defined role in the response to pathogens and is a regulator of keratinocyte growth and homeostasis [5, 6]. RIPK5, which is most similar to RIPK4, has no known role in innate immunity.

RIPK1 and RIPK3 are perhaps the best described members of the RIPK family and have critical roles in mediating cell death and inflammatory signaling [7]. Downstream of signals from innate immune receptors like Z-DNA binding protein 1 (ZBP1) and tumor necrosis factor receptor 1 (TNFR1), RIPK1 and/or RIPK3 are activated by autophosphorylation and proceed to activate additional effector proteins to carry out their innate immune functions. For example, RIPK3 can phosphorylate MLKL to activate highly inflammatory programmed necrotic cell death (necroptosis) [8], RIPK1/3 can engage caspase-8 (CASP8) to activate apoptotic caspases [9, 10], or RIPK1/3 can activate the pro-survival and pro-inflammatory transcription factor NF-κB [11, 12]. Several factors are known to impact the outcome of RIPK1/3 activation, such as the activating signal and caspase activity [7, 13]. Altogether, RIPK1 and RIPK3 are central to determining cell fate downstream of various innate immune stimuli.

Like many innate immune proteins, RIPK1 and RIPK3 are evolutionarily dynamic in vertebrates. Phylogenomic analyses of a small number of species from different vertebrate clades suggest that RIPK3, and the associated proteins ZBP1 and MLKL, have been lost in some vertebrate lineages including birds, carnivores, and marsupials [14, 15]. In addition, RIPK1, RIPK3, MLKL, and ZBP1 are known to interact with viral proteins

63 [16-21] and have been shown to be evolving under recurrent positive selection in both
64 primates and bats [22], a hallmark of host proteins that directly interact with viral proteins
65 [23]. The degree to which other RIP kinases (RIPK2, 4, and 5) and their interacting
66 partners have diversified across vertebrates is unknown. Moreover, the vast majority of
67 functional data on RIPKs are from human or mouse homologs, despite evolutionary
68 studies that suggest functional diversification in these proteins may have occurred.
69 Here, we use evolutionary and functional approaches to characterize RIPK1-5 and
70 their associated proteins across vertebrate species. We identify unique patterns of
71 conservation of RIP kinases and their associated proteins across vertebrate lineages.
72 These distinct evolutionary histories have resulted in different mechanisms of activation
73 of NF-κB for human RIPK1-4. In addition to observing the loss of RIPK3 and necroptosis-
74 associated proteins in some vertebrate lineages, we identify changes in regulatory
75 features—including catalytic sites and CASP cleavage sites—in RIPK1 and RIPK3 in
76 specific mammalian lineages that may affect their function. Intriguingly, we found that the
77 RIP homotypic interaction motif (RHIM) domain of RIPK1 and RIPK3, as well as other
78 RHIM-containing proteins, is highly conserved in vertebrates and in a non-vertebrate
79 RIPK1 protein. Consistent with this strong conservation of the RHIM domain, we found
80 that RIPK1 and RIPK3 proteins from diverse vertebrates, and even a non-vertebrate
81 RIPK1, are able to activate NF-κB in a RHIM-dependent manner, suggesting that
82 activation of this inflammatory response is a conserved function of RIPK1 and RIPK3 in
83 vertebrates. Altogether, these data suggest that activation of NF-κB is the ancestral and
84 conserved feature of RIP kinases, while other RIPK-mediated functions such as
85 necroptosis are more evolutionarily labile.
86
87 **Materials & Methods**
88 *Phylogenetic analysis*
89 Phylogenetic trees were generated for RIPK1-5 using previously described
90 methods [24]. Briefly, the kinase domains from human RIPK1 (NP_001341859.1), RIPK2
91 (NP_003812.1), RIPK3 (NP_006862.2), RIPK4 (NP_065690.2), and RIPK5
92 (NP_848605.1) were used to query the RefSeq protein database using BLASTp [25].
93 While LRRK1 and LRRK2 share kinase homology with RIPK1-5 and are sometimes

94 known as RIPK6 and -7 [3], they have a distinct domain structure and function compared
95 to RIPK1-5 and will therefore not be considered as RIP kinases for the purposes of this
96 study. The five resulting sequence lists were consolidated to a single list of unique
97 sequences using Geneious software. These sequences were then aligned using Clustal
98 Omega [26] with two refinement iterations implemented in Geneious software. Following
99 alignment, we filtered sequences based on alignment of an N-terminal kinase domain to
100 human RIPK kinase domains and the presence of a C-terminal domain. Proteins with
101 additional N-terminal domains, proteins lacking homology to human kinase domains, and
102 proteins lacking C-terminal domains were removed. Nearly-identical sequences were
103 reduced to a single unique sequence using CD-HIT [24] with a 0.8 sequence identity
104 cutoff. The resulting 736 sequences were realigned using Clustal Omega with two
105 refinement iterations. Phylogenetic trees were generated for both full length protein
106 alignments and for alignments trimmed to include only the kinase domains using IQ-TREE
107 [24] with 1000 bootstrap and SH-aLRT support values. The best substitution model was
108 determined by ModelFinder [27]. Accession numbers with species names and the tree
109 file can be found Supplementary Files 1 and 2.
110
111 *Gene loss analysis*
112 Using the aligned and filtered vertebrate RIPK sequences (4,550 sequences in
113 total, see 'Phylogenetic analysis' section), a tree was built using FastTree [28, 29]
114 implemented using Geneious. Using this tree, we were able to identify and extract *bona*
115 *fide* RIP kinases and remove similar, non-RIP kinases. The extracted sequences were
116 again aligned using Clustal Omega and filtered using the criteria above (See
117 'Phylogenetic analysis' section). A second tree was generated using FastTree. From this
118 tree, we extracted individual sequence lists for RIPK1-5 to determine which vertebrate
119 species did or did not have each RIPK. This method was repeated for CASP2 and
120 CASP8-10, ZBP1, MLKL, TRIF, FADD, NOD 1 and 2, and IRF6. The list of species and
121 lists of accession numbers for each protein can be found in Supplementary Files 3 and 4.
122
123 *Plasmids and constructs*

124 Coding sequences for human RIPK1 (Addgene #78834), human RIPK2
125 (ORFeome ID #4886), human RIPK3 (Addgene #78804), mouse RIPK1 (Addgene
126 #115341), and mouse RIPK3 (Addgene #78805) were cloned into apcDNA5/FRT/TO
127 backbone (Invitrogen, Carlsbad, CA) with an N-terminal V5 tag and linker using Gibson
128 Assembly (New England Biolabs, Ipswich, MA). Human RIPK4 (NP_065690.2) and
129 RIPK5 (NP_848605.1), and non-human RIPK1 C-termini (cat, XP_023109490.2; pig,
130 XP_003128209.1; chicken, NP_989733.3; lizard, XP_003224434.1; lamprey,
131 XP_032813622.1; zebra mussel, XP_052232845.1) and RIPK3 (cat, XP_003987615.3;
132 pig, XP_001927459.3; lizard, XP_003223896.2; turtle, XP_037771912.1; lamprey,
133 XP_032816533.1) homologues were ordered from Twist Biosciences (San Francisco,
134 CA, USA) and were cloned along with RHIM mutants targeting the core tetrad into the
135 pcDNA5/FRT/TO backbone (Invitrogen, Carlsbad, CA) with an N-terminal V5 tag and
136 linker using Gibson Assembly (New England Biolabs, Ipswich, MA). Kinase mutants for
137 human proteins RIPK1 (D138N), RIPK2 (D146N), RIPK3 (D142N), RIPK4 (D143N), and
138 RIPK5 (D145N), and RHIM mutants for RIPK1 (IQIG542AAAA) and RIPK3
139 (VQVG461AAAA) were generated using Gibson Assembly.
140
141 *Cell culture and transient transfections*
142 HEK293T cells (obtained from ATCC) and the generated HEK293T RIPK1 KO cells
143 were maintained at a low passage number to maintain less than one year since
144 purchase, acquisition, or generation. Both cell lines were grown in complete media
145 containing DMEM (Gibco, Carlsbad, CA), 10% FBS (Peak Serum, Wellington, CO), and
146 1% penicillin/streptomycin (Gibco, Carlsbad, CA). A day prior to transfection, HEK293T
147 and RIPK1 KO cells were seeded into 24-well plates with 500 µL complete media or 96-
148 well plates with 80 µL complete media. Cells were transiently transfected with 500 ng
149 total DNA and 1.5 µL of TransIT-X2 (Mirus Bio, Madison, WI) in 100 µL Opti-MEM
150 (Gibco, Carlsbad, CA) for a 24-well plate or 100 ng DNA and 0.3 µL TransIT-X2 in 10
151 µL Opti-MEM for a 96-well plate. DNA and TransIT-X2 were incubated at room
152 temperature for 25-30 minutes, then added dropwise to the appropriate well. Cells were
153 harvested or analyzed at 18-22 hours post-transfection.
154

155 *Generation of knockout cell lines*

156 RIPK1 knockout HEK293T cells were generated using CRISPR/Cas9 as
157 previously described [30, 31]. Briefly, plasmids were generated order to produce
158 lentivirus-like particles containing the CRISPR/Cas9 machinery and guide RNA targeting
159 exon 5 (ENSE00003586162) of RIPK1. The protocol for the molecular cloning of this
160 plasmid was adapted from Feng Zhang (Sanjana et al., 2014) using the transfer plasmid
161 pLB-Cas9 (gift from Feng Zhang, Addgene plasmid # 52962). We designed the gRNA
162 target sequence using the web tool CHOPCHOP (Labun et al., 2016), available at
163 https://chopchop.cbu.uib.no/, and synthesized oligonucleotides from Integrated DNA
164 Technologies (San Diego, CA). The synthesized oligonucleotide pair was phosphorylated
165 and annealed using T4 Polynucleotide Kinase (NEB M0201S) with T4 Ligation Buffer
166 (NEB). Duplexed oligonucleotides were ligated into dephosphorylated and BsmBI-
167 digested pLB-Cas9 using the Quick Ligase kit (NEB M2200S) to generate transfer
168 plasmid with RIPK1 guide sequence. To generate lentivirus-like particles, this transfer
169 plasmid was transfected alongside two packaging plasmids, pMD2.G (gift from Didier
170 Trono, Addgene plasmid # 12259) and psPAX2 (gift from Didier Trono, Addgene plasmid
171 # 12260), into HEK293T cells with a 1:1:1 stoichiometry. Forty-eight hours post-
172 transfection supernatant was harvested and syringe-filtered (0.45μm). Supernatant
173 containing sgRNA-encoding lentivirus-like particles was then used to transduce HEK293T
174 cells. Transduced cells were cultured in growth media for 48 hours, then cultured in
175 growth media supplemented with 1 μg/ml puromycin for 72 hours. Using limiting dilution
176 in 96-well plates, the monoclonal cell line was then obtained. RIPK1 knockout was
177 confirmed by Sanger sequencing and by western blot using an α-RIPK1 antibody.

178

179 *NF-κB and IFN luciferase reporter assays*

180 To quantify NF-κB and IFN activation, we used the Dual-Glo Luciferase Assay
181 System E2920 (Promega, USA). WT or RIPK1 KO HEK293T cells were seeded in a white
182 96-well plate and transfected with firefly luciferase fused to either the NF-κB response
183 element (pGL4.32, Promega) or the human IFN-beta promoter (IFN-Beta-pGL3, Addgene
184 #102597), renilla luciferase fused to herpes simplex virus thymidine kinase promoter
185 (pTK-Renilla, Thermo Scientific), and the indicated RIPK. Firefly luciferase was used as

186 the primary reporter with renilla luciferase being a normalization control. Eighteen to 24
187 hours after transfection, Dual-Glo Luciferase Assay Reagent was added to each
188 transfected well as well as 3-6 untransfected wells to serve as a negative control.
189 Following a 10-minute incubation, the firefly luciferase signal was measured using a
190 BioTek Cytation imaging reader with Gen5 software (Agilent Technologies, San Diego,
191 CA). Then, Dual-Glo Stop & Glo reagent was added to each well. Following a 10-minute
192 incubation, the renilla luciferase signal was measured. The background luminescence
193 signal from the buffer-treated untransfected conditions was subtracted from other
194 conditions, firefly values were normalized to renilla values, and all samples were
195 normalized to the empty vector control condition. Values are reported as NF-κB activity
196 (firefly/renilla).
197
198 *Cell death assay*
199 Cell viability was measured using the ReadyProbes Cell Viability Imaging Kit, Blue/Green
200 (ThermoFisher Scientific). HEK293T cells were seeded in 80 µL of DMEM+/+ (See "Cell
201 culture and transient transfections") in a clear 96-well plate and transfected with the
202 indicated plasmids or a vector control. Eighteen hours post-transfection, cells were
203 stained using NucBlue Live reagent, which stains all nuclei, and NucGreen Dead reagent,
204 which stains only dead cells. A 2x concentrated mix (4 drops/mL of each dye) was made
205 and added to wells to 1x concentration. Cells were incubated for 20 minutes at room
206 temperature. Fluorescence for NucBlue (DAPI, excitation 377/20, emission 447/20) and
207 NucGreen (GFP, excitation 469/20, emission 525/20) were read using a BioTek Cytation
208 imaging reader with Gen5 software (Agilent Technologies, San Diego, CA). Unstained
209 wells were read and used as controls for background fluorescence. GFP values were
210 normalized to DAPI values, and all samples were normalized to the vector control
211 condition. Values are reported as Cytotoxicity (GFP/DAPI).
212
213 *Immunoblotting and antibodies*
214 Eighteen to 22 hours post-transfection, cells were washed with 1X PBS and lysed with
215 boiling 1x NuPAGE LDS sample buffer containing 5% β-mercaptoethanol at room
216 temperature for 5 minutes and then at 98°C for 7-10 minutes. Lysates were separated

217 by SDS-PAGE (4-15% Bis-tris gel; Life Technologies, San Diego, CA) with 1X MOPS
218 buffer (Life Technologies, San Diego, CA). Proteins were transferred onto a
219 nitrocellulose membrane (Life Technologies, San Diego, CA) and blocked with PBS–T
220 containing 5% bovine serum albumin (BSA) (Spectrum, New Brunswick, NJ).
221 Membranes were incubated with the indicated rabbit primary antibodies diluted with 5%
222 BSA and PBS-T at 1:1000 overnight at 4°C (α-V5 clone D3H8Q, α-GAPDH clone
223 14C10, α-RIPK1 clone E8S7U XP, α-RIPK2 clone D10B11, α-RIPK3 clone E1Z1D, α-
224 RIPK4 #12636; Cell Signaling Technology, Danvers, MA). Membranes were rinsed
225 three times with PBS-T, incubated with HRP-conjugated rabbit secondary antibody
226 diluted at 1:10,000 with 5% BSA and PBS-T for 30 minutes at room temperature, and
227 developed with SuperSignal West Pico PLUS Chemiluminescent Substrate (Thermo
228 Fisher Scientific, Carlsbad, CA).
229
230 *Statistical analysis*
231 Statistical analyses were completed using GraphPad Prism 10 software. Tests were
232 performed as indicated. Error bars were calculated using SEM.
233
234 **Results**
235 *Comparative evolutionary and functional analysis of RIPK1-5*
236 To directly compare the evolution of all RIP kinases, we performed phylogenetic
237 analysis on RIPK1-5 in vertebrates. We analyzed both the full-length proteins (Figure 1A,
238 Supplementary Files 1 and 2) and the kinase domains (Supplementary Figure 1). RIPK1
239 and RIPK3 are closely related, as are RIPK4 and RIPK5, reflecting their similar C-terminal
240 domains (Figure 1B). Moreover, RIPK1, 3, and 5 have greater sequence diversity across
241 vertebrates when compared to more well conserved RIPK2 and RIPK4 (Figure 1C).
242 These data, which are consistent with prior data showing that RIPK1 and RIPK3 are
243 evolving under diversifying positive selection in two mammalian clades [22], indicate that
244 different selective pressures have shaped the evolution of different RIPK genes in
245 vertebrates.

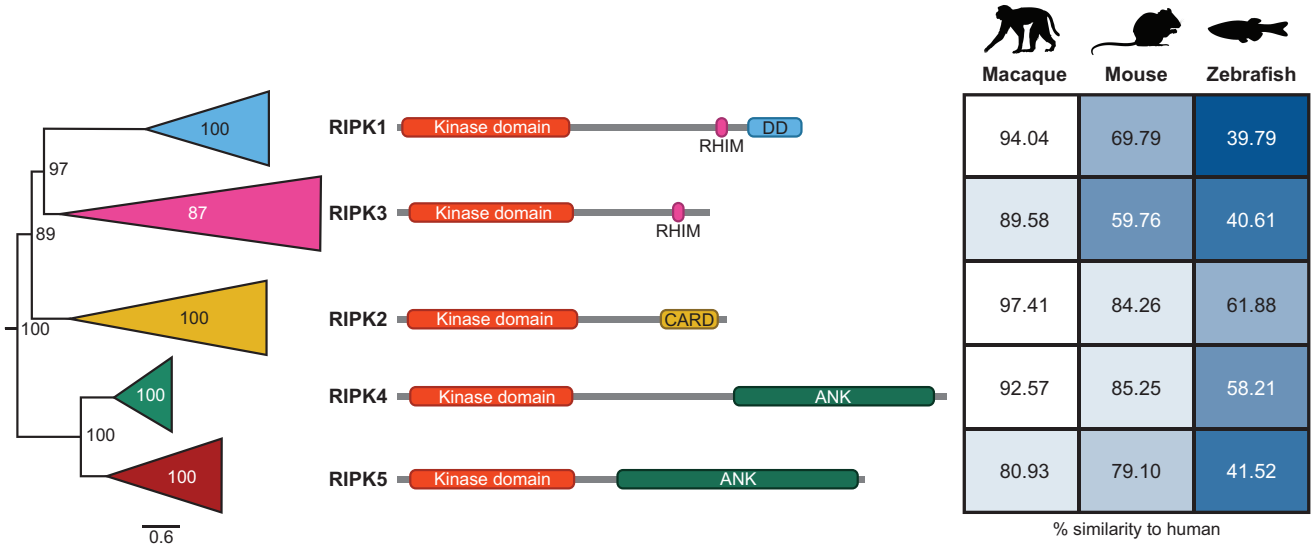

Figure 1: Diversity of RIPK evolution in vertebrates A) Maximum likelihood phylogenetic tree of vertebrate RIP kinases. The tree is rooted on an outgroup of RIPK proteins from *Petromyzon marinus* and cartilaginous fish. Bootstrap branch support values are indicated. The complete phylogenetic tree and list of protein accession numbers can be found in Supplementary Files 1 and 2. B) Domain structures of human RIP kinases. RHIM = RIP homotypic interaction motif, DD = death domain, CARD = caspase activation and recruitment domain, ANK = ankyrin repeats. C) Percent identity of macaque (*Macaca mulatta*), mouse (*Mus musculus*), and zebrafish (*Danio rerio*) RIP kinases compared to human proteins. Images of model species generated using BioRender.

RIPK1-4 have been reported to activate NF-κB in various cellular contexts while RIPK5 has no reported function in innate immune signaling [2]. We used a luciferase reporter assay to quantify activation of NF-κB by RIPK1-5 in HEK293T cells. As expected, overexpression of RIPK1-4 led to robust activation NF-κB (Figure 2A). In contrast, we observed no activation of NF-κB by RIPK5, despite expression levels similar to RIPK1 (Supplementary Figure 2). Interestingly, NF-κB activation by RIPK1-3 is independent of their kinase activity, while mutation of the RIPK4 kinase domain prevented activation of NF-κB (Figure 2B).

Of RIPK1-4, only RIPK1 is highly expressed in HEK293T cells (Supplementary Figure 3A-D). To better isolate the functions of individual RIP kinases, we generated *RIPK1* knockout HEK293T cells (RIPK1 KO; Supplementary Figure 3A, E). While RIPK2 and RIPK4 retained their ability to activate NF-κB, activation of NF-κB by RIPK3 is lost in RIPK1 KO cells (Figure 2C). This was expected given the critical role of RIPK1 in

regulating RIPK3 function [32]. These data suggest that the unique evolutionary histories of RIPK1-4 have led to distinct mechanisms for activation of NF-κB.

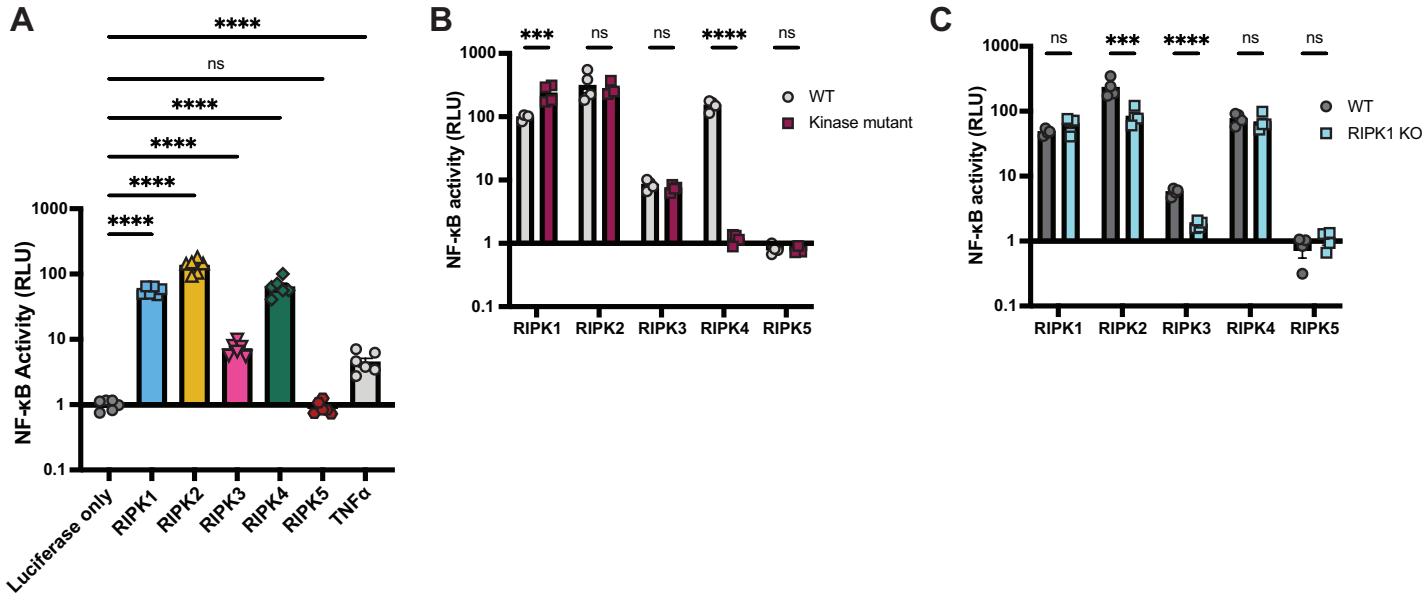

Figure 2: Differential mechanisms of NF-κB activation by human RIPK1-4. Human V5-RIPK1-5 proteins were transfected into WT (A-C) or RIPK1 KO (C) HEK293T cells, along with NF-κB firefly luciferase and control renilla luciferase reporter plasmids (see Materials and Methods), and NF-κB activity was measured at 18h post-transfection. A) Human RIPK1-5 activation of NF-κB in WT 293T cells. B) Activation of NF-κB by catalytically active versus kinase-mutant RIPK1-5 in WT HEK293T cells. C) Activation of NF-κB by RIPK1-5 in WT versus RIPK1 KO HEK293T cells) Data are representative of 3 independent experiments with n=3-6 replicates per group. Data were analyzed using one-way ANOVA with Dunnett's multiple comparisons test (A) or two-way ANOVA with Šidák's multiple comparisons test (B, C). ns = not significant, *** = p<0.001, **** = p<0.0001.

RIP kinases have also been reported to activate type I interferons (IFN-I) [33-35] and multiple forms of cell death [7]. Overexpression of RIPK2 and RIPK4 lead to moderate IFN-I activation (Supplementary Figure 4A), which has been previously reported for RIPK2 but not RIPK4 [33], although the overall activation was <1% the level of activation seen upon overexpression of MAVS (mitochondrial antiviral signaling protein). Only RIPK1 was able to induce any cell death over background levels (Supplementary Figure 4B) indicative of its central role in regulating cell survival and death [36], although this is also minimal compared to a known activator of cell death. In contrast, RIPK3, which on its own does not induce cell death, potently induces cell death when co-expressed with ZBP1 and MLKL (Supplementary Figure 4B-C) [8, 37]. Altogether, these data highlight

293 the diverse functions of human RIPK1-4, as well as the conserved function of NF-κB
294 activation.
295
296 *Phylogenomic analysis of RIPK and associated proteins in vertebrates*
297 RIPK3, ZBP1, and MLKL are known to be lost in some vertebrate lineages [14]. It
298 is unknown if other RIPK and RIPK-associated proteins are similarly lost. We therefore
299 performed phylogenomic analysis on 490 vertebrate species for the presence or absence
300 of RIPK1-5 and several key RIPK-associated proteins (Figure 3, Supplementary Files 3
301 and 4). Due to the difficulty in discerning whether a gene absence in an individual species
302 is due to true gene loss or incomplete genome assembly, we focused on multi-species
303 patterns of gene loss within and between vertebrate lineages. We first confirmed the loss
304 of necroptosis associated proteins that has been previously reported [14]: RIPK3 and
305 ZBP1 in birds; RIPK3, ZBP1, and MLKL in marsupials; MLKL in carnivores. ZBP1 is
306 absent in fish, suggesting that this protein, and ZBP1-mediated necroptosis, arose only
307 during tetrapod evolution. Analysis of other RIP kinases revealed that RIPK1, RIPK2, and
308 RIPK4 are found in most jawed vertebrate species, while RIPK5 is recurrently lost in
309 different vertebrate lineages similar to RIPK3. Moreover, RIPK1-3 are found in the most
310 distant vertebrate species, relative to humans, sea lamprey (*Petromyzon marinus*),
311 whereas RIPK4 and RIPK5 are absent in this deeply branched vertebrate species.
312 Intriguingly, we observed a second paralog of RIPK2, which we call RIPK2B, in many
313 vertebrates but lost in therian (live-bearing) mammals (Supplementary Figure 5).
314 Additionally, we found a RIPK1-like protein in several non-vertebrate species, including
315 the zebra mussel *Dreissena polymorpha*. Additional RIPK-like proteins have been found
316 in other non-vertebrate species, including a RIPK1/2-like protein in *Drosophila* and other
317 protostomes [14], although these proteins were not considered here due to minimal
318 sequence similarity to the human RIP kinase domains and our focus on vertebrate RIP
319 kinases. Together, these data indicate that RIP kinases have duplicated, diversified, and,
320 in the cases of RIPK3 and RIPK5, have been recurrently lost throughout vertebrate
321 evolution.

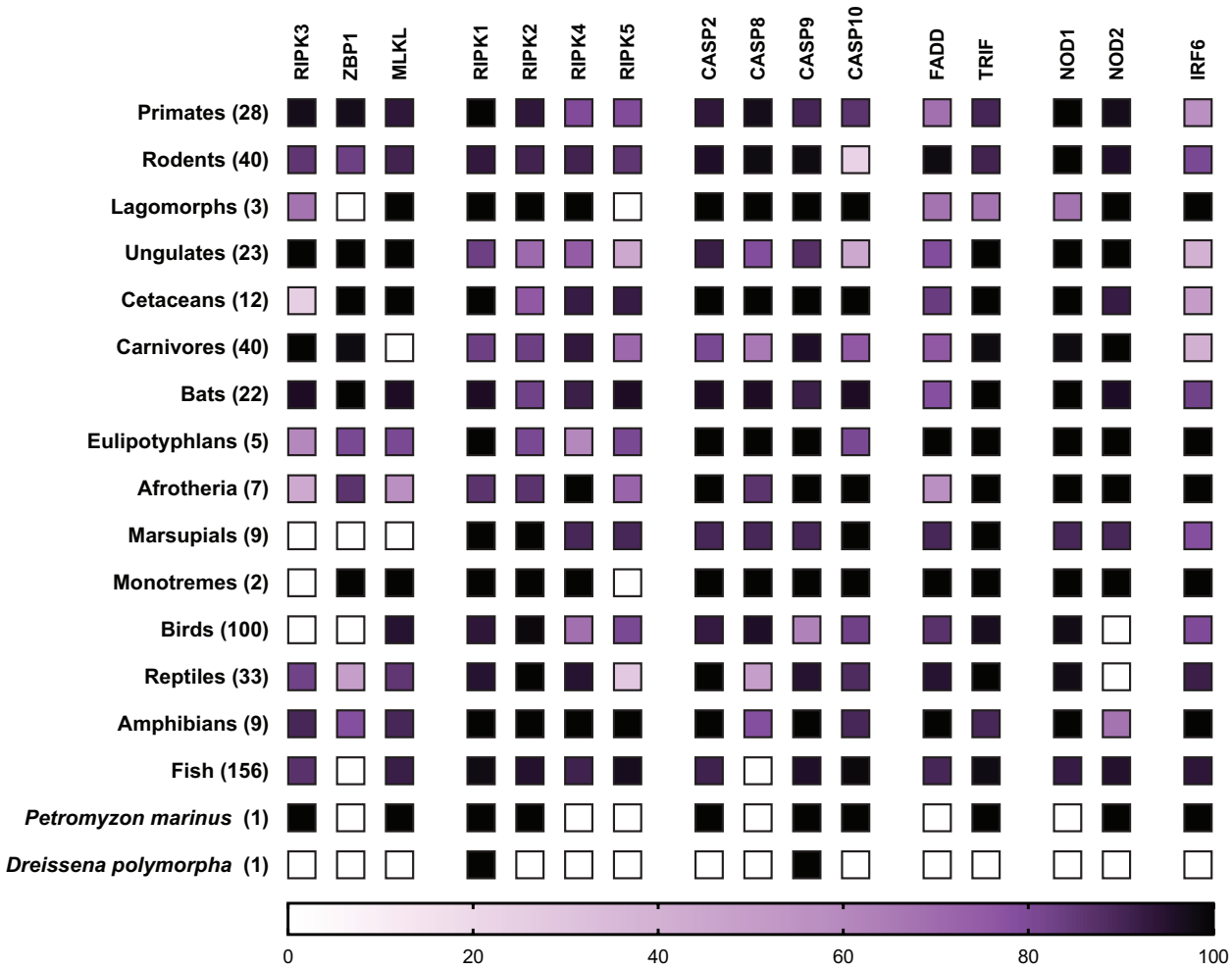

Figure 3: Loss of specific RIPK and associated proteins in some vertebrate lineages. Heat map showing the percentage of species within a clade that have the indicated protein. The clades and the number of species within each clade are indicated on the left. Complete lists of proteins and species in each group can be found in Supplementary Files 3 and 4.

We also analyzed the phylogenomic distribution of other RIPK-associated proteins. We analyzed caspase-8 (CASP8) and additional activator caspases CASP2, CASP9, and CASP10. We confirmed the loss of CASP10 in some rodents [38], revealing that suborder Myomorpha (“mouse-like”) and Castorimorpha (“beaver-like”) rodents have lost CASP10, whereas Sciuromorpha (“squirrel-like”) and Hystricomorpha (“porcupine-like”) rodents have retained CASP10. We found that CASP8 is absent in fish and sea lamprey. This coincides with the emergence of ZBP1 in tetrapods. Further supporting the link between CASP8 and ZBP1, CASP8 is lost in some reptiles that have also lost ZBP1 (Supplementary Table 1). CASP8 is a known negative regulator of necroptosis and is important for mitigating ZBP1-induced inflammation [39]. These data suggest that loss of

338 ZBP1 is sufficient to allow for loss of CASP8. In contrast to CASP8, FADD, which may
339 also contribute to regulation of ZBP1 activity [39], is found in all jawed vertebrates,
340 indicating that it emerged prior to ZBP1. Additional RIPK-associated proteins, including
341 TRIF (RIPK1-interacting), NOD 1 and NOD2 (RIPK2-interacting), and IRF6 (RIPK4-
342 interacting) were also analyzed [1, 2]. TRIF is broadly expressed across vertebrates.
343 NOD1 is only found in jawed vertebrates. NOD2 is present in lamprey and fish, but absent
344 in birds, reptiles, and some amphibians, including some of the same species that contain
345 RIPK2B, the paralog of RIPK2 (Supplementary Figure 5). While RIPK2B retains both the
346 kinase domain and CARD, there may be distinct regulatory mechanisms, specifically
347 those related to NOD2, compared to RIPK2. Altogether, our large-scale phylogenomic
348 analysis revealed patterns of conservation and evolutionary lability in RIPK and RIPK-
349 associated proteins in vertebrates.
350
351 *Lineage-specific losses of RIPK functional motifs despite broad conservation of RHIM*
352 *domains across vertebrates*
353 In addition to analyzing the presence or absence of a protein across vertebrates,
354 we characterized the presence of specific regulatory and functional sites within proteins,
355 including catalytic sites, phosphorylation sites, and caspase cleavage sites. For instance,
356 the known CASP8 cleavage site in RIPK1 is absent in many cetaceans (Figure 4A).
357 Cetaceans have been shown to have disrupted necroptosis through truncation of RIPK3
358 (identified here as a loss of RIPK3) [15], suggesting that CASP8 cleavage of RIPK1 in
359 these species is likely not necessary to regulate necroptosis. However, there could be
360 other CASP cleavage sites within these RIPK1 proteins that serves a similar regulatory
361 function. Interestingly, while RIPK3 is retained in carnivores, the key catalytic residue
362 (D142 in human RIPK3), is mutated to an asparagine (Figure 4B). This, combined with
363 the loss of MLKL in carnivores, suggests that the role of RIPK3 in this order is independent
364 of its kinase activity.
365 Interestingly, despite the loss of key functional domains of RIPK1 and RIPK3, the
366 core tetrad of the RHIM domain (V/I-Q-V/I-G), is conserved across vertebrates (Figure
367 4C-F). This motif has been shown to be important for RIPK1-RIPK3 interactions, and
368 facilitates known kinase-independent functions of RIPK3 [40]. Moreover, the first RHIM

369 domain of ZBP1 and the TRIF RHIM domain are also highly conserved in vertebrates
370 (Supplementary Figure 6A, left and 6B). Interestingly, the second RHIM domain of ZBP1
371 diverges outside of mammals (Supplementary Figure 6A, right). Altogether, the strong
372 conservation of the RHIM domain across RIPK1 and RIPK3, despite the loss of other
373 functional motifs, suggests the ancestral and conserved functions of these proteins are
374 RHIM-dependent.

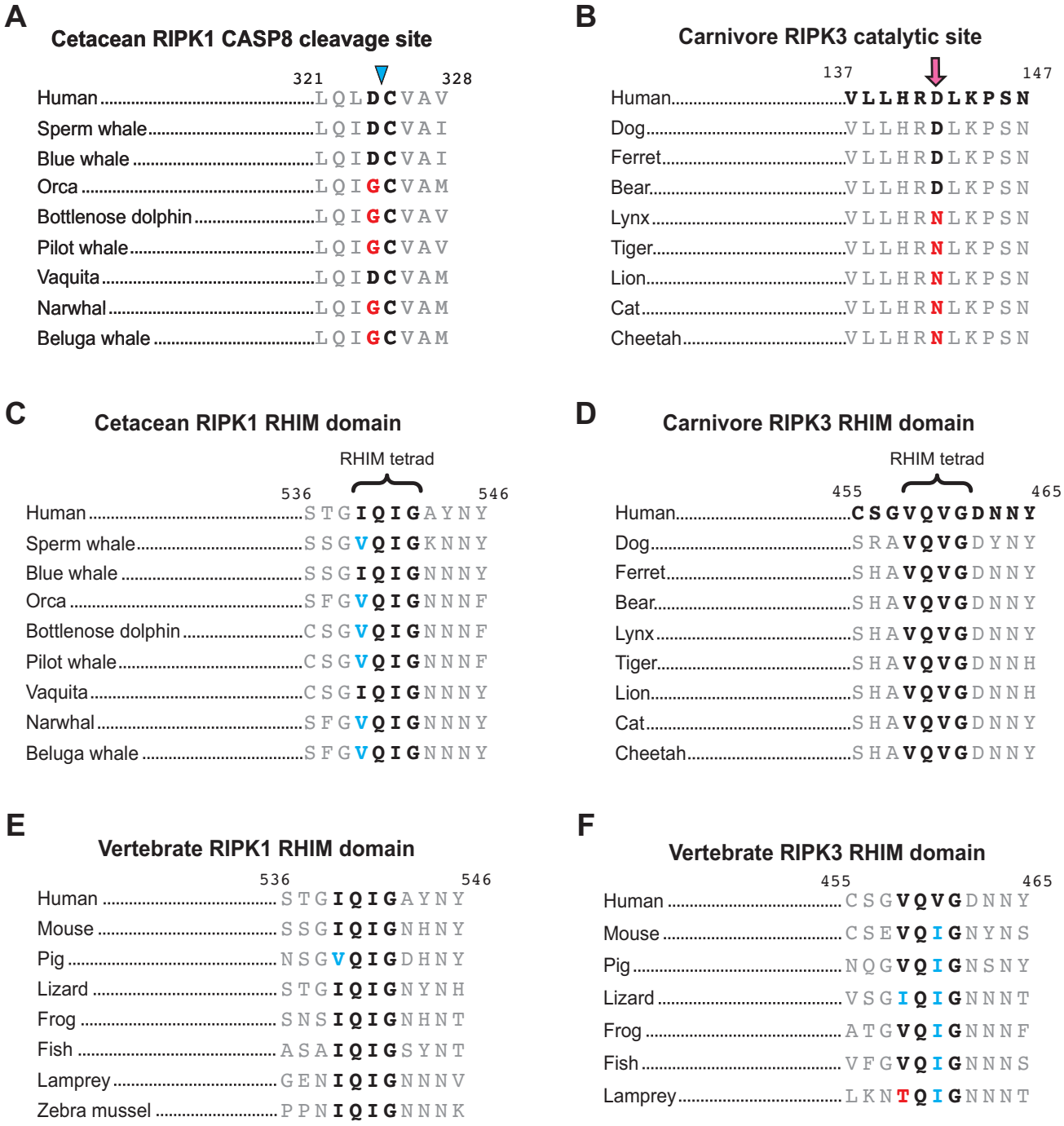

375

Figure 4: Conservation of the RIPK1 and RIPK3 RHIM domain across vertebrates. RIPK1 sequences from cetaceans highlighting the CASP8 cleavage site (A) and the RHIM tetrad (C). RIPK3 sequences from carnivore species highlighting the catalytic site in the kinase domain (B) and the RHIM tetrad (D). The RHIM domain of RIPK1 (E) and RIPK3 (F) from diverse vertebrate species. Residue numbers refer to the human sequence. Cetacean species include sperm whale (*Physeter catodon*), blue whale (*Balaenoptera musculus*), orca (*Orcinus orca*), bottlenose dolphin (*Tursiops truncatus*), pilot whale (*Globicephala melas*), vaquita (*Phocoena sinus*), narwhal (*Monodon monoceros*), and beluga whale (*Delphinapterus leucas*). Carnivore species include dog (*Canis lupus familiaris*), ferret (*Mustela putorius furo*), bear (*Ursus americanus*), lynx (*Lynx canadensis*), tiger (*Panthera tigris*), lion (*Panthera leo*), cat (*Felis catus*), cheetah (*Acinonyx jubatus*). RIPK3 (B) and RIPK1 (C) sequences from vertebrate species highlighting the core tetrad of the RHIM domain. Residue numbers refer to the human sequence. Vertebrate species shown include mouse (*Mus musculus*), bat (*Pteropus alecto*), pig (*Sus scrofa*), cat (*Felis catus*), lizard (*Anolis carolinensis*), frog (*Xenopus laevis*), fish (*Danio rerio*), lamprey (*Petromyzon marinus*), and zebra mussel (*Dreissena polymorpha*).

RHIM-dependent NF-κB activation by RIPK1 and RIPK3 is conserved in vertebrates

Activation of NF-κB by RIPK3 is dependent on the presence of RIPK1 (Figure 2C). We hypothesized this is due to direct interaction with RIPK1 via the RHIM domain. We therefore tested for activation of NF-κB by a RIPK3 RHIM mutant. Activation of NF-κB by RIPK3 is completely ablated upon mutation of the RHIM core tetrad (Supplementary Figure 7A). Interestingly, while mutation of the RIPK1 RHIM domain reduces activation of NF-κB, there is still robust activation (Supplementary Figure 7A). This is likely due to death domain-mediated interactions. We also tested NF-κB activation of other RHIM-containing proteins. As described previously [41], ZBP1 activates NF-κB in a RHIM- and RIPK1-dependent manner (Supplementary Figure 7B-C), although only the first RHIM is required for activation. Conversely, mutation of the TRIF RHIM domain does not affect activation of NF-κB, and activation is only moderately reduced in RIPK1 KO cells (Supplementary Figure 7D-E), likely due to the TIR domain in TRIF that is known mediate its innate immune signaling [40].

The strong conservation of the RHIM domain tetrad sequence (V/I-Q-V/I-G) of RIPK1 and RIPK3 across species led us to hypothesize that activation of NF-κB by RIPK1 and RIPK3 is also conserved. We therefore decided to tested a diverse panel of metazoan RIPK1 proteins in our NF-κB assay. To avoid the effects of both kinase activity and kinase-mediated interactions [42], we generated RIPK1 C-terminus ($RIPK1^{CT}$) proteins from diverse species (Supplementary Figure 8A). Both WT and RHIM mutant $RIPK1^{CT}$ activate NF-κB to the same extent as full length RIPK1 (Supplementary Figure 8B).

413 Mammalian and non-mammalian RIPK1^{CT} proteins were all able to activate NF-κB
414 independently of endogenous RIPK1 (Figure 5A, Supplementary Figure 9). Similar to
415 human RIPK1, mutation of the RHIM domain does not affect activation of NF-κB by other
416 mammalian proteins, including mouse, cat, and pig (Figure 5B, left). In contrast, mutation
417 of the RHIM domain attenuated the ability of lizard and zebra mussel RIPK1^{CT} to activate
418 NF-κB, and mutation of the lamprey RHIM domain completely prevented activation of NF-
419 κB (Figure 5B, right).

420 We then tested diverse RIPK3 proteins for activation of NF-κB, including species
421 that do (mouse, pig, turtle) and do not (cat, lizard, sea lamprey) have a complete
422 necroptosis pathway as defined by presence of ZBP1, MLKL, and catalytically active
423 RIPK3. Mouse and cat RIPK3 activated NF-κB in a RIPK1-dependent manner, while pig
424 RIPK3 did not activate NF-κB (Figure 5C, left, Supplementary Figure 10). We additionally
425 tested the ability of mammalian RIPK3 to activate cell death using human ZBP1 and MLKL
426 (Supplementary Figure 11). Interestingly, pig RIPK3 activated cell death despite being
427 unable to activate NF-κB. Conversely, cat RIPK3 failed to activate cell death
428 (Supplementary Figure 11), confirming its catalytic inactivity, but is able to activate NF-
429 κB (Figure 5C, left). These data suggest that activation of cell death and NF-κB are two
430 distinct functions of RIPK3. Both lizard and turtle RIPK3 were able to activate NF-κB
431 independent of RIPK1 (Figure 5C, right). Activation of NF-κB was dependent on the RHIM
432 domain for all RIPK3 proteins tested, regardless of their dependence on RIPK1 (Figure
433 5D). Sea lamprey RIPK3, which has a RHIM tetrad of TQIG, had limited activation of NF-
434 κB, but activation increased upon insertion of a IQIG tetrad (Figure 5D). This highlights
435 the importance of the RHIM domain, particularly the core tetrad, in driving activation of
436 NF-κB. Altogether, these data reveal the conservation of NF-κB activation by vertebrate
437 RIPK1 and RIPK3 via the RHIM domain, while also highlighting subtle differences
438 between mammalian and non-mammalian RIP kinases.

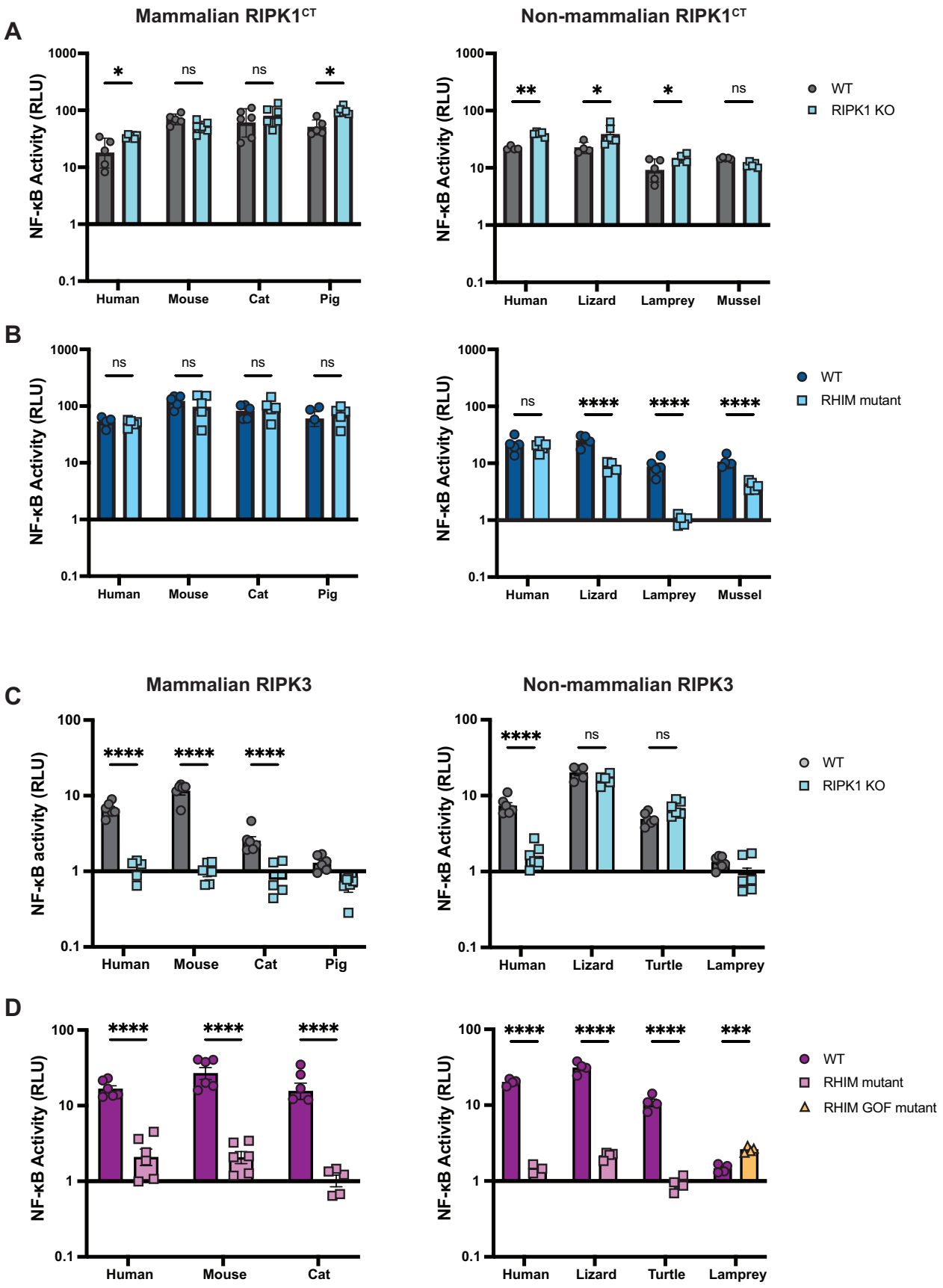
A
Mammalian RIPK1CT
Non-mammalian RIPK1CT
NF-κB Activity (RLU)
1000
100
10
1
0.1
*
ns
ns
*
Human
Mouse
Cat
Pig
**
*
*
ns
Human
Lizard
Lamprey
Mussel
WT
RIPK1 KO
B
ns
ns
ns
ns
ns
****
****
****
WT
RHIM mutant
C
Mammalian RIPK3
Non-mammalian RIPK3
NF-κB activity (RLU)
****
****
****
Human
Mouse
Cat
Pig
****
ns
ns
Human
Lizard
Turtle
Lamprey
WT
RIPK1 KO
D
****
****
****
Human
Mouse
Cat
****
****
****
***
Human
Lizard
Turtle
Lamprey
WT
RHIM mutant
RHIM GOF mutant

439

Figure 5: NF-κB activation is a conserved function of RIPK1 and RIPK3 across vertebrates. RIPK1^{CT} (A-B) or RIPK3 (C-D) proteins were transfected into WT or RIPK1 KO HEK293T cells, along with NF-κB firefly luciferase and control renilla luciferase reporter plasmids (see Materials and Methods), and NF-κB activity was measured at 18h post-transfection A) Activation of NF-κB by mammalian (left) and non-mammalian (right) RIPK1^{CT} in WT and RIPK1 KO HEK293T cells. B) Activation of NF-κB by WT and RHIM mutant mammalian (left) and non-mammalian (right RIPK1^{CT} in WT HEK293T cells. C) Activation of NF-κB by mammalian (left) and non-mammalian (right) RIPK3 in WT and RIPK1 KO HEK293T cells. D) Activation of NF-κB by WT and RHIM mutant mammalian (left) and non-mammalian (right) RIPK3 in HEK293T cells. Squares in (D) represent inactivating alanine mutations, triangles represent a gain of function TQIG>IQIG mutation. Species shown are mouse (*Mus musculus*), cat (*Felis catus*), pig (*Sus scrofa*), lizard (*Anolis carolinensis*), turtle (*Chelonia mydas*), lamprey (*Petromyzon marinus*), and mussel (*Dreissena polymorpha*). Data are representative of 3-5 independent experiments with n=3-6 replicates per group. Data were analyzed using two-way ANOVA with Šidák's multiple comparisons test. ns = not significant* = $p<0.05$, ** = $p<0.01$, *** = $p<0.001$, **** = $p<0.0001$.

Discussion

Activation of NF-κB is critical to both the innate and adaptive immune response in humans and mice [43]. NF-κB and analogous pathways have been found in many non-vertebrate species, including horseshoe crab [44], *Drosophila melanogaster* [45], and cnidarians and bivalves (reviewed in [46]). Despite this deep conservation of NF-κB signaling, differences in the function and regulation of NF-κB-associated proteins between mice and humans have been identified [43], suggesting that this functionally well-conserved pathway can be adapted to different species. These data indicate that broader phylogenetic analysis of the genes and functions that are associated with NF-κB signaling are needed to understand the pathogen response across species, including those that harbor viruses and bacteria that pose a zoonotic threat to humans.

Here, we apply broad phylogenetic and functional sampling to the RIP kinase family of NF-κB activators. Using a phylogenomic approach, we identified widespread conservation of RIPK1, RIPK2, and RIPK4 within vertebrates. We also show conservation of activation of NF-κB signaling by RIPK1 and RIPK3 across diverse vertebrate species that is reliant on the highly conserved core tetrad of the RHIM domains found in both proteins. This striking conservation of RIPK1- and RIPK3-mediated activation of NF-κB, from species that span >500 million years of vertebrate evolution, underscores the core functionality of RIP kinases as NF-κB activating proteins. Despite this conservation of NF-κB activation, we also observed lineage specific changes in RIPK presence or mechanisms of NF-κB activation. For instance, we observed recurrent gene loss of RIPK3

477 and RIPK5 throughout the vertebrate phylogeny, and discovered a second paralog of
478 RIPK2 in many non-mammalian vertebrate species (RIPK2B). In addition, although
479 RIPK3-mediated activation of NF-κB is highly dependent on RIPK1 across diverse
480 mammals, RIPK3 activation of NF-κB in reptiles is independent of RIPK1. Activation of
481 NF-κB is part of the antiviral immune response and is known to be antagonized by viruses
482 across a range of species, including vertebrates and non-vertebrates [47-49]. This
483 antagonism could result in adaptation of NF-κB-associated proteins, including RIP
484 kinases, leading to lineage-specific mechanisms of activation that are tailored to the
485 specific contexts within and between species.

486 The most striking differences in RIPK-associated genes and functions are those
487 involved in necroptosis. Necroptosis is highly inflammatory and the associated proteins
488 must therefore be tightly regulated, as it could be a cause of immunopathology during
489 infection. Despite this, necroptosis has been shown to be important for the response to
490 several viruses [50-52]. It is hypothesized that necroptosis, defined by RIPK3-mediated
491 activation of MLKL, arose in vertebrates [14, 53]. Interestingly, we find that two critical
492 regulators of necroptosis, CASP8 and ZBP1, are only found in tetrapods, suggestive of
493 an additional innovation within the necroptosis pathway during the divergence of
494 tetrapods. Moreover, consistent with previous observations [14, 15], we observe a large
495 number of necroptosis-associated gene losses, while also discovering important
496 functional motifs in necroptosis proteins in distinct tetrapod lineages. These data support
497 a model where necroptosis has been constructed as an important facet of the innate
498 immune response in some tetrapods, but is not universal and has been deconstructed in
499 species where the immunopathologic effects outweigh the benefits.

500 There have been several hypotheses to explain the loss of necroptosis associated
501 proteins in specific vertebrate lineages, such as diet (*e.g.,* carnivores) or behavior (*e.g.,*
502 torpor in reptiles) [14]. While the cause of a specific instance of gene loss is difficult to
503 identify, it is clear that gene loss can provide an evolutionary tool for adaptation [54].For
504 example, caspases, which are key regulators of both immunologically silent apoptosis
505 and inflammatory pyroptosis, differ greatly across mammals, with lineage-specific
506 caspase repertoires including both loss and gain of novel caspases [38]. Even within a
507 single mammalian order, homologous caspases have been found to serve different

508 functions in response to pathogens [55]. This type of lineage-specific innovation likely
509 exists for necroptosis, and gene loss could be a cause or a result of adaptations. Indeed,
510 differences in MLKL activation by RIPK3 across species have been identified [56], which
511 may be the result of additional diverse regulatory mechanisms for necroptosis even
512 amongst species with an intact pathway. Strikingly, despite the lack of a complete
513 necroptosis pathway in some lineages (cat, turtle, lamprey), our functional data indicate
514 that RIPK3 retains the ability to activate NF-κB. Activation of NF-κB could therefore
515 represent the ancestral function of RIPK3, and it has been co-opted to activate
516 necroptosis in vertebrates.

517 Altogether, our combined phylogenetic and functional approaches reveal both
518 conservation and a striking lack of conservation in vertebrate RIPKs and their associated
519 proteins and functions. The strong conservation of RIPK1 proteins and their ability to
520 activate NF-κB across species is consistent with the model in which RIPK1 function is
521 central to determining cell fate downstream of TNF and TLR signaling [36]. Indeed, RIPK1
522 has been described as a guardian of antimicrobial proinflammatory signaling, where
523 RIPK1 activates proinflammatory and pro-survival signals downstream of multiple innate
524 immune receptors as a way to preserve activation in the face of pathogen antagonism
525 [57]. For instance, because some pathogens have evolved strategies to inhibit CASP8,
526 RIPK1- and RIPK3-mediated necroptosis is activated as a secondary cell death strategy
527 when CASP8 is inhibited [57]. This places both RIPK1 and RIPK3, a critical regulator of
528 necroptosis, at the center of determining cell fate during pathogen infection. The
529 divergence of RIPK1 and RIPK3 across vertebrates identified here, as well as the
530 previous finding that these proteins are evolving under positive selection [15, 22], may
531 have also resulted in distinct regulatory mechanisms or functions of these proteins across
532 species, such as the loss of the CASP8 cleavage site in some cetacean RIPK1 proteins
533 identified here. Thus, the functional divergence identified in our work highlights the
534 evolutionary innovation that can arise in innate signaling pathways across diverse
535 species, and underscores the importance of considering natural diversity when
536 characterizing the innate immune response to pathogens.
537

538 **References**

1. Cuny, G.D. and A. Degterev, *RIPK protein kinase family: Atypical lives of typical kinases.* Semin Cell Dev Biol, 2021. **109**: p. 96-105.
2. Eng, V.V., M.A. Wemyss, and J.S. Pearson, *The diverse roles of RIP kinases in host-pathogen interactions.* Semin Cell Dev Biol, 2021. **109**: p. 125-143.
3. Lv, S., et al., *Comparative and evolutionary analysis of RIP kinases in immune responses.* Front Genet, 2022. **13**: p. 796291.
4. Meylan, E., et al., *RIP4 (DIK/PKK), a novel member of the RIP kinase family, activates NF-kappa B and is processed during apoptosis.* EMBO Rep, 2002. **3**(12): p. 1201-8.
5. Kwa, M.Q., G.M. Scholz, and E.C. Reynolds, *RIPK4 activates an IRF6-mediated proinflammatory cytokine response in keratinocytes.* Cytokine, 2016. **83**: p. 19-26.
6. Kwa, M.Q., et al., *Receptor-interacting protein kinase 4 and interferon regulatory factor 6 function as a signaling axis to regulate keratinocyte differentiation.* J Biol Chem, 2014. **289**(45): p. 31077-87.
7. Newton, K., *RIPK1 and RIPK3: critical regulators of inflammation and cell death.* Trends Cell Biol, 2015. **25**(6): p. 347-53.
8. Sun, L., et al., *Mixed lineage kinase domain-like protein mediates necrosis signaling downstream of RIP3 kinase.* Cell, 2012. **148**(1-2): p. 213-27.
9. Wang, L., F. Du, and X. Wang, *TNF-alpha induces two distinct caspase-8 activation pathways.* Cell, 2008. **133**(4): p. 693-703.
10. Mandal, P., et al., *RIP3 induces apoptosis independent of pronecrotic kinase activity.* Mol Cell, 2014. **56**(4): p. 481-95.
11. Meylan, E., et al., *RIP1 is an essential mediator of Toll-like receptor 3-induced NF-kappa B activation.* Nat Immunol, 2004. **5**(5): p. 503-7.
12. Moriwaki, K., et al., *The necroptosis adaptor RIPK3 promotes injury-induced cytokine expression and tissue repair.* Immunity, 2014. **41**(4): p. 567-78.
13. Orozco, S. and A. Oberst, *RIPK3 in cell death and inflammation: the good, the bad, and the ugly.* Immunol Rev, 2017. **277**(1): p. 102-112.
14. Dondelinger, Y., et al., *An evolutionary perspective on the necroptotic pathway.* Trends Cell Biol, 2016. **26**(10): p. 721-732.
15. Agueda-Pinto, A., et al., *Convergent Loss of the Necroptosis Pathway in Disparate Mammalian Lineages Shapes Viruses Countermeasures.* Front Immunol, 2021. **12**: p. 747737.
16. Harris, K.G., et al., *RIP3 Regulates Autophagy and Promotes Coxsackievirus B3 Infection of Intestinal Epithelial Cells.* Cell Host Microbe, 2015. **18**(2): p. 221-32.
17. Croft, S.N., E.J. Walker, and R. Ghildyal, *Human Rhinovirus 3C protease cleaves RIPK1, concurrent with caspase 8 activation.* Sci Rep, 2018. **8**(1): p. 1569.
18. Wagner, R.N., J.C. Reed, and S.K. Chanda, *HIV-1 protease cleaves the serine-threonine kinases RIPK1 and RIPK2.* Retrovirology, 2015. **12**: p. 74.
19. Muscolino, E., et al., *Species-Specific Inhibition of Necroptosis by HCMV UL36.* Viruses, 2021. **13**(11).
20. Huang, Z., et al., *RIP1/RIP3 binding to HSV-1 ICP6 initiates necroptosis to restrict virus propagation in mice.* Cell Host Microbe, 2015. **17**(2): p. 229-42.

583 21. Liu, X., et al., *Epstein-Barr virus encoded latent membrane protein 1 suppresses*
584 *necroptosis through targeting RIPK1/3 ubiquitination.* Cell Death Dis, 2018. **9**(2):
585 p. 53.
586 22. Palmer, S., et al., *Evolutionary profile for (host and viral) MLKL indicates its*
587 *activities as a battlefront for extensive counteradaptation.* Mol Biol Evol, 2021.
588 **38**(12): p. 5405-522.
589 23. Daugherty, M.D. and H.S. Malik, *Rules of engagement: molecular insights from*
590 *host-virus arms races.* Annu Rev Genet, 2012. **46**: p. 677-700.
591 24. Fu, L., et al., *CD-HIT: accelerated for clustering the next-generation sequencing*
592 *data.* Bioinformatics, 2012. **28**(23): p. 3150-2.
593 25. Altschul, S.F., et al., *Gapped BLAST and PSI-BLAST: a new generation of protein*
594 *database search programs.* Nucleic Acids Res, 1997. **25**(17): p. 3389-402.
595 26. Sievers, F., et al., *Fast, scalable generation of high-quality protein multiple*
596 *sequence alignments using Clustal Omega.* Mol Syst Biol, 2011. **7**: p. 539.
597 27. Kalyaanamoorthy, S., et al., *ModelFinder: fast model selection for accurate*
598 *phylogenetic estimates.* Nat Methods, 2017. **14**(6): p. 587-589.
599 28. Price, M.N., P.S. Dehal, and A.P. Arkin, *FastTree: computing large minimum*
600 *evolution trees with profiles instead of a distance matrix.* Mol Biol Evol, 2009. **26**(7):
601 p. 1641-50.
602 29. Price, M.N., P.S. Dehal, and A.P. Arkin, *FastTree 2--approximately maximum-*
603 *likelihood trees for large alignments.* PLoS One, 2010. **5**(3): p. e9490.
604 30. Tsu, B.V., et al., *Diverse viral proteases activate the NLRP1 inflammasome.* Elife,
605 2021. **10**.
606 31. Stevens, D.A., et al., *Antiviral function and viral antagonism of the rapidly evolving*
607 *dynein activating adaptor NINL.* Elife, 2022. **11**.
608 32. Liu, S., et al., *RIPK3 signaling and its role in the pathogenesis of cancers.* Cell Mol
609 Life Sci, 2021. **78**(23): p. 7199-7217.
610 33. Pandey, A.K., et al., *NOD2, RIP2 and IRF5 play a critical role in the type I interferon*
611 *response to Mycobacterium tuberculosis.* PLoS Pathog, 2009. **5**(7): p. e1000500.
612 34. Lei, Y., et al., *Cooperative sensing of mitochondrial DNA by ZBP1 and cGAS*
613 *promotes cardiotoxicity.* Cell, 2023. **186**(14): p. 3013-3032 e22.
614 35. Saleh, D., et al., *Kinase Activities of RIPK1 and RIPK3 Can Direct IFN-beta*
615 *Synthesis Induced by Lipopolysaccharide.* J Immunol, 2017. **198**(11): p. 4435-
616 4447.
617 36. Clucas, J. and P. Meier, *Roles of RIPK1 as a stress sentinel coordinating cell*
618 *survival and immunogenic cell death.* Nat Rev Mol Cell Biol, 2023. **24**(11): p. 835-
619 852.
620 37. Upton, J.W., W.J. Kaiser, and E.S. Mocarski, *DAI/ZBP1/DLM-1 complexes with*
621 *RIP3 to mediate virus-induced programmed necrosis that is targeted by murine*
622 *cytomegalovirus vIRA.* Cell Host Microbe, 2012. **11**(3): p. 290-7.
623 38. Eckhart, L., et al., *Identification of novel mammalian caspases reveals an important*
624 *role of gene loss in shaping the human caspase repertoire.* Mol Biol Evol, 2008.
625 **25**(5): p. 831-41.
626 39. Rodriguez, D.A., et al., *Caspase-8 and FADD prevent spontaneous ZBP1*
627 *expression and necroptosis.* Proc Natl Acad Sci U S A, 2022. **119**(41): p.
628 e2207240119.

629 40. Nanson, J.D., B. Kobe, and T. Ve, *Death, TIR, and RHIM: Self-assembling*
630 *domains involved in innate immunity and cell-death signaling.* J Leukoc Biol, 2019.
631 **105**(2): p. 363-375.
632 41. Rebsamen, M., et al., *DAI/ZBP1 recruits RIP1 and RIP3 through RIP homotypic*
633 *interaction motifs to activate NF-kappaB.* EMBO Rep, 2009. **10**(8): p. 916-22.
634 42. Delanghe, T., Y. Dondelinger, and M.J.M. Bertrand, *RIPK1 Kinase-Dependent*
635 *Death: A Symphony of Phosphorylation Events.* Trends Cell Biol, 2020. **30**(3): p.
636 189-200.
637 43. Zhang, Q., M.J. Lenardo, and D. Baltimore, *30 Years of NF-kappaB: A Blossoming*
638 *of Relevance to Human Pathobiology.* Cell, 2017. **168**(1-2): p. 37-57.
639 44. Wang, X.W., et al., *Evidence for the ancient origin of the NF-kappaB/IkappaB*
640 *cascade: its archaic role in pathogen infection and immunity.* Proc Natl Acad Sci U
641 S A, 2006. **103**(11): p. 4204-9.
642 45. Hetru, C. and J.A. Hoffmann, *NF-kappaB in the immune response of Drosophila.*
643 Cold Spring Harb Perspect Biol, 2009. **1**(6): p. a000232.
644 46. Williams, L.M. and T.D. Gilmore, *Looking Down on NF-kappaB.* Mol Cell Biol,
645 2020. **40**(15).
646 47. Albarnaz, J.D., et al., *Molecular mimicry of NF-kappaB by vaccinia virus protein*
647 *enables selective inhibition of antiviral responses.* Nat Microbiol, 2022. **7**(1): p.
648 154-168.
649 48. Gonzalez Lopez Ledesma, M.M., et al., *Dengue virus NS5 degrades ERC1 during*
650 *infection to antagonize NF-kB activation.* Proc Natl Acad Sci U S A, 2023. **120**(23):
651 p. e2220005120.
652 49. Palmer, W.H., et al., *Induction and Suppression of NF-kappaB Signalling by a DNA*
653 *Virus of Drosophila.* J Virol, 2019. **93**(3).
654 50. Koehler, H., et al., *Vaccinia virus E3 prevents sensing of Z-RNA to block ZBP1-*
655 *dependent necroptosis.* Cell Host Microbe, 2021. **29**(8): p. 1266-1276 e5.
656 51. Balachandran, S. and G.F. Rall, *Benefits and Perils of Necroptosis in Influenza*
657 *Virus Infection.* J Virol, 2020. **94**(9).
658 52. Shubina, M., et al., *Necroptosis restricts influenza A virus as a stand-alone cell*
659 *death mechanism.* J Exp Med, 2020. **217**(11).
660 53. Tummers, B. and D.R. Green, *The evolution of regulated cell death pathways in*
661 *animals and their evasion by pathogens.* Physiol Rev, 2022. **102**(1): p. 411-454.
662 54. Albalat, R. and C. Canestro, *Evolution by gene loss.* Nat Rev Genet, 2016. **17**(7):
663 p. 379-91.
664 55. Devant, P., A. Cao, and J.C. Kagan, *Evolution-inspired redesign of the LPS*
665 *receptor caspase-4 into an interleukin-1beta converting enzyme.* Sci Immunol,
666 2021. **6**(62).
667 56. Tanzer, M.C., et al., *Evolutionary divergence of the necroptosis effector MLKL.* Cell
668 Death Differ, 2016. **23**(7): p. 1185-97.
669 57. Remick, B.C., M.M. Gaidt, and R.E. Vance, *Effector-Triggered Immunity.* Annu
670 Rev Immunol, 2023. **41**: p. 453-481.
671